

THERMODYNAMIC PROPERTIES OF THE LIPID BILAYER TRANSITION

Pseudocritical Phenomena

SHIGEKI MITAKU, TOSHIYO JIPPO, AND RYOICHI KATAOKA

Tokyo University of Agriculture and Technology, Faculty of Technology, Department of Material Systems Engineering, Nakamachi, Koganei, Tokyo 184, Japan

ABSTRACT Ultrasonic relaxation of multilamellar liposomes formed from dipalmitoylphosphatidylcholine was measured near the gel-to-liquid crystal transition by a differential ultrasonic resonator. The relaxation time and strength increased remarkably near the transition temperature, indicating a pseudocritical phenomenon. A quantitative analysis of the relaxation in terms of thermodynamic relationships between specific heat, thermal-expansion coefficient, and compressibility showed that more than 90% of the total endothermic heat of the transition arises from the latent heat. The temperature dependence of the ultrasonic relaxation parameters was also analyzed by the Landau theory; we obtain a small but finite difference, 0.6°C, between the pseudocritical temperature and the transition temperature. These results provide a quantitative description of both the first-order and second-order characters of the gel-to-liquid crystal transition.

INTRODUCTION

Both the physical and biological aspects of the lipid bilayer transition have attracted much interest, and the nature of this transition has been studied by measuring a variety of its properties. The experimental data available at present indicate that the transition has both first and second-order characteristics. On the one hand, sharp changes are observed in various physical properties like specific heat (1), density (2), intramolecular vibration (3), orientational order of hydrocarbon chains (4, 5), intermolecular and intermembrane distances (6), lateral diffusion constant (7), and partitioning of a nitroxide-spin label (8). These abrupt changes in physical properties are due to the isothermal first-order transition. On the other hand, a broad anomalous peak or dip is found near the transition temperature in ultrasonic velocity and absorption (9, 10), permeability (11), relaxation times in various time ranges (12, 13), and two-dimensional compressibility (14). This kind of anomaly is usually observed when structural fluctuation is enhanced as in the second-order phase transitions. Therefore the gel-to-liquid crystal transition of the lipid bilayer is considered a weak first-order transition that shows latent heat as well as pseudocritical anomalies.

Then a naive question arises—how close to a hidden critical point is the gel-to-liquid crystal transition, or how large are the first-order isothermal changes compared to the pseudocritical anomalies? Quantitative analysis of the temperature dependence of various physical properties is

required to answer this question. For example, the thermal heat capacity of a weak first-order transition is characterized by an isothermal endothermic heat, i.e., the latent heat, accompanied by a broad anomalous enhancement of the specific heat. When the transition is very close to a second-order transition, the latent heat has to be small compared with the contribution of pseudocritical anomalies. The determination of a pseudocritical temperature, which is defined as a point of the divergence of various thermodynamic properties, also provides an answer to this question, because the difference between the pseudocritical temperature, T^* , and the transition temperature, T_i , disappears at the critical point (15, 16).

Both the specific heat anomaly due to the pseudocritical phenomena and the pseudocritical temperature can be determined from ultrasonic measurements if the complete frequency dependence of the ultrasonic velocity and absorption, which yield the relaxation strength and relaxation time, are available. The specific heat anomaly due to the pseudocritical phenomena is obtained according to its proportionality to the anomalous part of the compressibility deduced from the ultrasonic relaxation strength as first shown by Pippard for the λ transition (17). The subtraction of this contribution from the total endothermic heat has to give the latent heat, allowing a quantitative comparison between the first-order and second-order characters of the gel-to-liquid crystal transition. The pseudocritical temperature is easily determined from the ultrasonic measurements if we assume a critical exponential dependence of

the relaxation parameters on the temperature. This assumption is considered quite reasonable and has been successfully used to study various phase transitions (18).

We describe here the first quantitative analysis of the first-order as well as second-order characters of the gel-to-liquid crystal transition using the ultrasonic technique. We have developed an ultrasonic resonator that measures the ultrasonic velocity dispersion and absorption of dilute membrane suspensions and measured a suspension of dipalmitoylphosphatidylcholine multilamellar liposomes. The specific heat anomaly was calculated from the ultrasonic relaxation strength, leading to the conclusion that more than 90% of the endothermic heat is the latent heat. We have also analyzed the temperature dependence of the ultrasonic relaxation strength and relaxation time with critical exponents of the molecular-field theory (15, 16, 19). The temperature dependence of the relaxation parameters was described very well with the Landau theory and indicated that $T_i - T^* = 0.6^\circ\text{C}$.

MATERIALS

Multilamellar liposomes were prepared from 1- α -dipalmitoylphosphatidylcholine (Sigma Chemical Co., St. Louis, MO) as described before (9). In this work, however, we dispersed liposomes by mild shaking at $\sim 50^\circ\text{C}$ to prevent the formation of small lipid vesicles, which show broader transition behaviors. The concentration of lipid was 2.48-mg dry weight/ml in 5-mM sodium phosphate buffer (pH 7.3).

METHODS

Measurement of Ultrasonic Relaxation

Ultrasonic relaxation was measured by a differential ultrasonic resonator that was developed for the simultaneous measurement of ultrasonic velocity and absorption in the frequency range between 1 and 8 MHz (20). This apparatus has much higher accuracy of the ultrasonic velocity measurement than previous ultrasonic resonators. Although only the ultrasonic absorption was previously measured by an ultrasonic resonator because of the poor accuracy of the ultrasonic velocity measurement, the ultrasonic velocity is necessary for the accurate determination of the

relaxation strength as well as the relaxation time. The high accuracy was realized by the least square analysis of ultrasonic resonance curves as follows. The output voltage, U , from the receiving transducer is related to the frequency, f (20, 21),

$$U = U_{\max} \left[1 + \frac{\sin^2(2\pi f \ell / V - \phi)}{\sinh^2(\mu f \ell / V)} \right]^{-1/2}, \quad (1)$$

where V and μ represent the ultrasonic velocity and absorption per wavelength, respectively. Therefore if we plot $s[(U_{\max}/U)^2 - 1]^{-1/2}$ ($s = 1$ for $f > f_{\max}$, and $s = -1$ for $f < f_{\max}$) as a function of frequency, f , near a resonance peak, Eq. 1 is linearized as shown in Fig. 1. The resonance frequency that is proportional to the ultrasonic velocity is obtained precisely from the intersection at f -axis by the least-square analysis. The accurate measurement of velocity was difficult in former ultrasonic resonator instruments, but the linearized plot of Eq. 1 enabled us to make the measurements with an accuracy of 1×10^{-5} for the velocity and 5×10^{-5} for the absorption.

Analysis of Ultrasonic Relaxation

The analysis was performed in terms of limiting numbers of the velocity, $[V]$, and the absorption per wavelength, $[\mu]$.

$$[V] = \lim_{c \rightarrow 0} \frac{V - V_s}{V_s c} = [V]_0 + \Delta \frac{\omega^2 \tau^2}{1 + \omega^2 \tau^2}, \quad (2)$$

$$[\mu]/2\pi = \lim_{c \rightarrow 0} \frac{\mu - \mu_s}{2\pi c} = B\omega + \Delta \frac{\omega\tau}{1 + \omega^2 \tau^2}. \quad (3)$$

Here, $[V]_0$ is the limiting number of the velocity at the low frequency limit, Δ and τ are the relaxation strength and relaxation time, respectively, and B corresponds to the classical contribution of viscosities. We have determined the relaxation parameters by least-square fitting of Eqs. 2 and 3 to the experimental data, assuming that $B = 5 \times 10^{-11} \text{ cm}^3/\text{g}$. This value of B corresponds to the membrane viscosity of $\sim 2 \text{ P}$ (22). This correction term is so small that the change in B does not cause any essential difference in our analysis.

The limiting number of the velocity is a linear function of the compressibility of the membrane,

$$[V] = -\frac{1}{2} \left(\frac{\kappa_m - \kappa_s}{\kappa_s} + \frac{\rho_m - \rho_s}{\rho_s} \right) \frac{1 + \delta}{\rho_m}, \quad (4)$$

where the suffixes m and s denote the membrane and solvent, κ and ρ represent compressibility and density, respectively, and δ is the amount of water of hydration per 1 g of membrane. Only the membrane compressibility, κ_m , may have a relaxation term in Eq. 4. Therefore the expression for the relaxation strength is directly derived from Eq. 4

$$\Delta = \frac{\Delta\kappa_m}{2\kappa_s} \cdot \frac{1 + \delta}{\rho_m}. \quad (5)$$

RESULTS

We have measured the ultrasonic relaxation of multilamellar dipalmitoylphosphatidylcholine (DPPC) liposomes near the gel-to-liquid crystal transition. Typical relaxation curves are shown in Fig. 2. The theoretical curves indicate that the relaxation is well approximated by a single-relaxation time (Eqs. 2 and 3). As discussed previously (13), the calculated relaxation parameters, Δ and τ , have little ambiguity, because we used both the ultrasonic velocity and absorption. When either of the ultrasonic

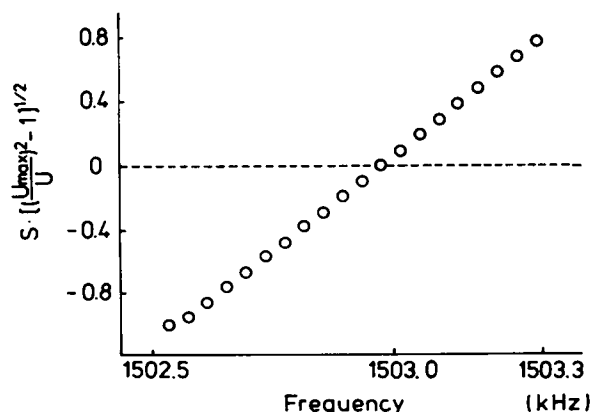


FIGURE 1 Linearized plot of an ultrasonic resonance peak at 1.5 MHz. With the least-squares analysis of this plot a relative accuracy of 10^{-5} was achieved for the ultrasonic velocity measurement throughout the frequency range from 1 to 8 MHz.

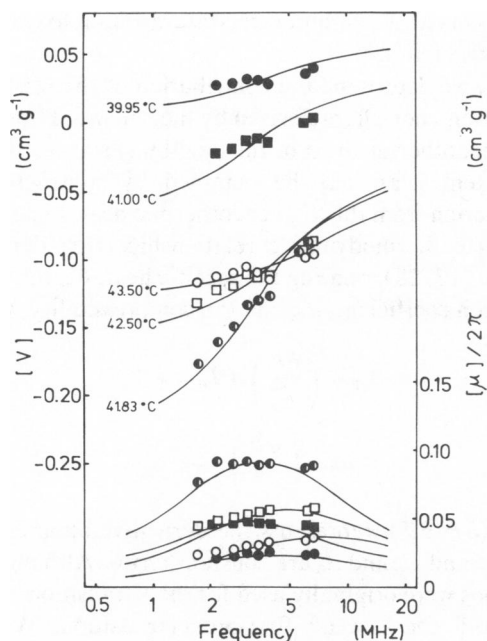


FIGURE 2 Ultrasonic relaxation curves of L- α -dipalmitoylphosphatidylcholine liposomes (2.48 mg/ml) at various temperatures: (●), 39.95°C; (■), 41.00°C; (●), 41.83°C; (□), 42.50°C; and (○), 43.50°C. Upper and lower curves correspond to the limiting numbers of the velocity and the absorption, respectively. The solid lines are the single-relaxation curves best fitted to experimental data by a least-square analysis.

propagation constants is not available, the relaxation parameters may have a large error; poor accuracy is expected for the relaxation time without a velocity measurement and for the relaxation strength without an absorption measurement. Fig. 2 clearly indicates the pseudocritical anomalies of the gel-to-liquid crystal transition, which may be summarized as follows. (a) The ultrasonic velocity at low frequencies shows an anomalous dip (critical softening). (b) The ultrasonic absorption has a maximum at the transition temperature, corresponding to the relaxation strength. (c) The relaxation time is longest at the transition temperature (critical slowing down).

The anomalous behavior of the relaxation strength, Δ , and the relaxation time, τ , are shown in Figs. 3 and 4. The previous results for sonicated small vesicles are plotted for comparison. The relaxation strength exceeds $0.2 \text{ cm}^3/\text{g}$ at the transition temperature. This indicates that the relaxation strength of the compressibility of membrane is as large as $1.5 \times 10^{-11} \text{ cm}^2/\text{dyn}$, which corresponds to almost 40% of the membrane compressibility. Also shown in Fig. 3 is the scale for the compressibility, which was calculated by Eq. 5 on the assumption that $\kappa_s = 4.2 \times 10^{-11} \text{ cm}^2/\text{dyn}$, $\rho_m = 1.1 \text{ g/cm}^3$, and $\delta = 0.4$. These assumptions are reasonable in a narrow temperature region near the transition point (13). The shape of the anomaly is asymmetric with respect to the transition point, which is consistent with the results of thermal analysis and density measurement (1, 2).

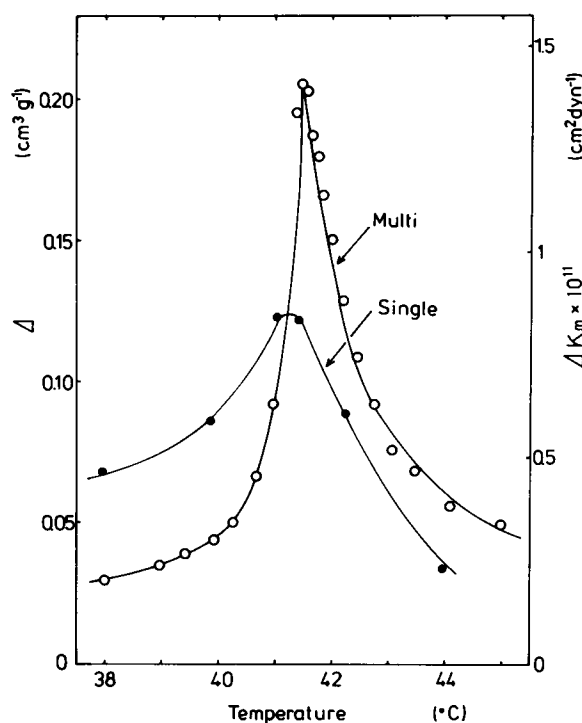


FIGURE 3 Relaxation strength as a function of temperature. ○, nonsonicated multilamellar liposomes; ●, the previous result obtained with sonicated small vesicles (13).

The relaxation time increases from ~ 15 to 60 ns , when the temperature approaches the transition temperature. This fact seems to indicate that the ultrasonic relaxation is directly coupled to the relaxation of membrane order. The value of the relaxation time is larger than the rotational-relaxation time of a single lipid molecule by one or two orders of magnitude (4). Therefore the relaxation process

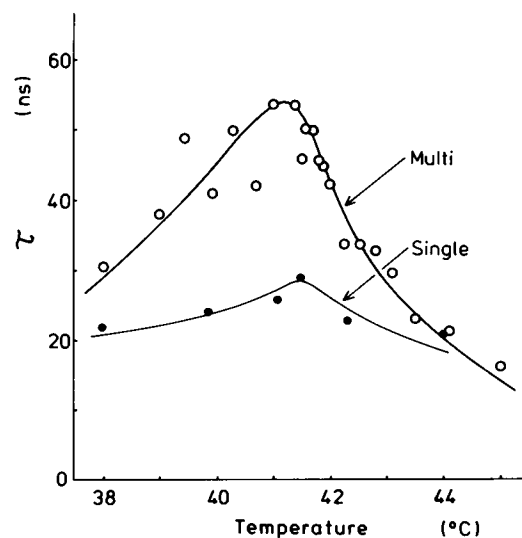


FIGURE 4 Relaxation time as a function of temperature. ○, nonsonicated multilamellar liposomes; ●, the previous result obtained with sonicated small vesicles (13).

observed by the ultrasonic measurement has to involve a large number of lipid molecules, in accord with the concept of the order parameter that is defined in a semimicroscopic volume. Furthermore, the relaxation time of 10–60 ns is in good agreement with the relaxation time of nematic order in the nematic-isotropic transition (23). Therefore we assume that the ultrasonic relaxation in this work is directly related to the fluctuation and relaxation of the membrane order.

Rounding of the anomalous peak is observed particularly in the relaxation time. A plausible cause of the rounding seems to be the contamination of small vesicles, although we have tried to get rid of them by avoiding vigorous shaking. The effect of vesicle size on the relaxation properties is remarkable (24, 25). The maximum values of the relaxation strength as well as the relaxation time of sonicated small vesicles are only half of the corresponding values of multilamellar liposomes. Particularly, the anomalous peak of the relaxation time is smeared out by the sonication. When we consider the transition properties, this size effect is important, because the rounding of the peak apparently removes the first-order character. The agreement of the transition temperature of the sonicated vesicles with that of the multilamellar liposomes appears to contradict previous experiments (25) that show a lowering of the transition temperature by sonication. However, this was apparently due to the conventional definition of the transition temperature in previous work; it was defined as the midpoint of a sigmoidal change, which is not necessarily a transition point as in the case of magnetic transitions (9, 13).

DISCUSSION

The qualitative features of the results, the anomalous softening and slowing-down, lead to the conclusion that the gel-to-liquid crystal transition is accompanied by an increased fluctuation near the transition temperature, as discussed previously (9, 13, 20). A qualitative discussion may be outlined as follows. The compressibility of the membrane has a sharp peak near the transition temperature as shown in Fig. 3. Isothermal compressibility, κ_T , is generally proportional to the mean square of the density fluctuation $\langle \delta\rho^2 \rangle$ in a semimicroscopic volume, v , (15),

$$\kappa_T = \frac{\langle \delta\rho^2 \rangle}{v k_B T \rho^2}, \quad (6)$$

where k_B represents the Boltzmann constant. Therefore the compressibility anomaly in Fig. 3 indicates that the fluctuation of density is anomalously enhanced near the transition temperature. This argument on the ultrasonic anomalies has revealed that the gel-to-liquid crystal transition is very nearly a second-order phase transition, in accord with theoretical work (19, 26, 27). In the present work, therefore, we concentrate our discussion on the quantitative

analysis of the gel-to-liquid crystal transition to clarify this qualitative feature.

First, we determine the contribution of the pseudocritical phenomenon characterized by the enhanced fluctuation to the endothermic heat of the lipid bilayer transition. The true latent heat may be obtained by subtracting this contribution from the total endothermic heat. In doing this, we utilize thermodynamic relationships first derived by Pippard (17, 28), relating the specific heat, C_p , the thermal expansion coefficient, α_p , and the compressibility, κ_T .

$$C_p = \left(\frac{\partial P}{\partial T} \right)_i V T_i \alpha_p + C_0, \quad (7)$$

$$\alpha_p = \left(\frac{\partial P}{\partial T} \right)_i \kappa_T + \alpha_0, \quad (8)$$

where $(\partial P/\partial T)_i$ represents the derivative along a transition line and C_0 and α_0 are constant terms. Although these equations were originally used for the λ transition, they are also valid for a weak first-order transition. When we consider only the anomalous parts, the constant terms may be neglected,

$$\Delta C_p = \left(\frac{\partial P}{\partial T} \right)_i V T_i \Delta \alpha_p, \quad (9)$$

$$\Delta \alpha_p = \left(\frac{\partial P}{\partial T} \right)_i \Delta \kappa_T. \quad (10)$$

The experimental value of $(\partial P/\partial T)_i$ was reported by Trudell et al. (29), as 46 kbar/deg, which permits the calculation of the specific heat anomaly ΔC_p from $\Delta \alpha_p$ or $\Delta \kappa_T$. The anomalous part of the compressibility in Fig. 3 certainly arises from the pseudocritical phenomenon, because the measuring frequency is so high that no isothermal structural change takes place. On the other hand, the specific heat anomaly from direct measurement, as well as from $\Delta \alpha_p$, has to contain isothermal contributions. The specific heat anomaly calculated from $\Delta \kappa_m$ is shown in Fig. 5 together with the similar calculation from $\Delta \alpha_p$ (30) and the direct measurement of ΔC_p by a differential scanning calorimeter (DSC) (1, 30). In the calculation of $\Delta \alpha_p$ and ΔC_p from the data of Wilkinson and Nagle (30), the anomalous part was determined assuming that the temperature dependence above 60°C is the base line free from the transition anomaly. When $\Delta T > 5^\circ\text{C}$, all the data agree fairly well, considering the poor accuracy of measurements in this temperature range. This indicates that these quantities are thermodynamically consistent and reasonable, assuring the validity of Eqs. 7 and 8 in the lipid bilayer transition.

The most striking difference between the specific heat derived from the direct measurements and the value calculated from $\Delta \kappa_m$ is the magnitude of the endothermic heat. The peak height of ΔC_p by the direct measurement is almost 60 times larger than the calculated value from $\Delta \kappa_m$.

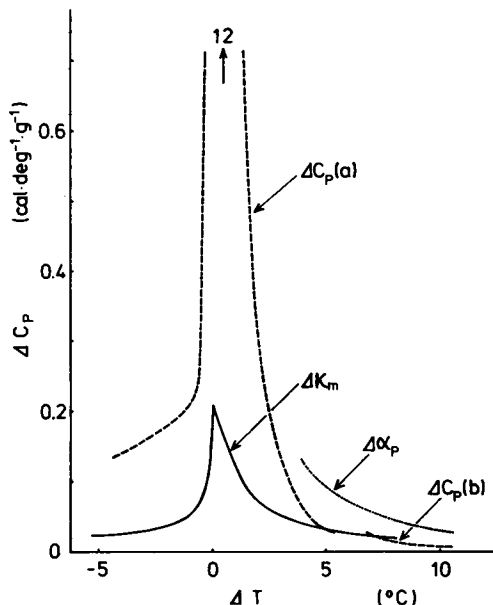


FIGURE 5 Anomalies of the specific heat in the vicinity of the transition temperature. ---, ΔC_p (a) from reference 1 and —, ΔC_p (b) from reference 27 were measured by a differential scanning calorimeter. The estimation of the specific-heat anomaly from $\Delta \kappa_m$, —, and $\Delta \alpha_p$, ···, (30) was performed using Pippard's relation (Eqs. 7 and 8). Appropriate base lines were assumed for ΔC_p (b) and $\Delta \alpha_p$ extrapolating from more than 20°C above the transition temperature.

The anomalous part of compressibility is determined from the relaxation strength in the frequency region of several megahertz; therefore the specific heat anomaly calculated from $\Delta \kappa_m$ is free from the contribution of the latent heat whose relaxation time is much longer than 1 μ s. On the other hand, the apparent specific-heat anomaly by DSC is the sum of the contribution from the pseudocritical phenomenon and the latent heat, which is isothermal in principle but shows a finite width due to the finite-scan speed of temperature. The true latent heat, ΔH_l may be obtained by subtracting the integration of the specific-heat anomaly, ΔH_a , which is ~ 0.6 kcal/mol, from the total endothermic heat, ΔH , of 8.7 kcal/mol. The latent heat of 8.1 kcal/mol obtained in this way indicates that a large fraction of the endothermic heat is the latent heat. Because $\Delta \kappa_m$ is the adiabatic compressibility instead of the isothermal compressibility used in Eq. 10 and the integration was performed in a limited temperature range of $-8^\circ\text{C} < \Delta T < 20^\circ\text{C}$, there is some ambiguity in the estimation of the latent heat. However, the latent heat should account for the greater part of the endothermic heat.

Integrating Eq. 10, we may also estimate from $\Delta \kappa_m$ the volume change of the membrane during the gel-to-liquid crystal transition. The result indicated that $\Delta V/V = 1.6 \times 10^{-3}$. This corresponds to the volume change due to the pseudocritical phenomenon. Comparing this value with the total volume change, 3.5×10^{-2} (2), the isothermal volume change at the transition temperature is calculated to be

3.3×10^{-2} . When we calculate the latent heat from the isothermal volume change by the Clausius-Clapeyron relation using a reasonable assumption of the molar volume of a lipid bilayer, 720 cm^3 (24),

$$Q = \left(\frac{\partial P}{\partial T} \right)_{T_i} \Delta V \quad (11)$$

the value of 8.0 kcal/mol is obtained, in good agreement with 8.1 kcal/mol estimated above. Consequently, all thermodynamic quantities that are available at present are in accord with thermodynamic relations, Eqs. 7–11, and indicate that more than 90% of the endothermic heat as well as volume change is of an isothermal nature. Nevertheless, note also that the contribution of the pseudocritical anomaly, $\Delta H_a = 0.6$ kcal/mol, is four times larger than the total endothermic heat, ΔH , of the nematic-isotropic transition (31).

Next, we analyze the temperature dependence of the relaxation parameters. Near the transition temperature, the fluctuation of the lipid bilayer structure is enhanced between gel and liquid crystalline phases. It is phenomenologically due to the broadening of the free-energy trough as well as the lowering of the energy barrier between two phases that cause a marked decrease of the effective restoring force as the order parameter fluctuates around the equilibrium value. In the framework of the Landau theory of phase transitions, the free energy of a system is expanded by the powers of an order parameter, η , to describe this behavior of free energy,

$$F(P, T, \eta) = F_0(P, T) + \frac{1}{2} A_2 \eta^2 - \frac{1}{3} A_3 \eta^3 + \frac{1}{4} A_4 \eta^4, \quad (12)$$

where A_2 is linearly related to temperature, $A_2 = a(T - T^*)$ (32, 33). When $A_3 = 0$, the free-energy barrier separating two phases disappears at the transition point and the pseudocritical temperature, T^* , in the liquid crystalline phase coincides with the transition temperature, T_i . Namely, the transition becomes second order.

Thermodynamic fluctuation of the order parameter in the disordered phase is easily calculated from Eq. 12. The effective force constant against the deviation of the order parameter from the equilibrium is equal to A_2 in the disordered phase, which vanishes at T^* . Hence the magnitude of fluctuation, $\langle \delta \eta^2 \rangle$, and the relaxation time, τ , of the order parameter diverge near T^* .

$$\langle \delta \eta^2 \rangle = \frac{k_B T}{a(T - T^*)}, \quad (13)$$

$$\tau = \frac{\zeta}{a(T - T^*)}, \quad (14)$$

where ζ is a kinetic coefficient (34). By analyzing experimental data of ultrasonic relaxation in Eqs. 13 and 14, we determined the pseudocritical temperature in the liquid

crystalline phase. The reciprocals of the relaxation time and the relaxation strength of multilamellar liposomes of dipalmitoylphosphatidylcholine are plotted as a function of temperature in Fig. 6. Although considerable rounding is observed near T_i , the linear relations indicate that the temperature dependence of the relaxation parameters is expressed well by Eqs. 13 and 14. $\Delta = 0.186/(T - 40.8)$, $\tau = 6.75 \times 10^{-8}/(T - 40.8)$.

The pseudocritical temperature, T^* , was 40.8°C. Because the transition temperature, T_i , is in the range from 41.3 to 41.5°C, as determined by the peaks of the compressibility, relaxation time and strength, $(T_i - T^*)$ is $\sim 0.6^\circ\text{C}$. The finite value of $(T_i - T^*)$ again leads to the conclusion that the gel-to-liquid crystal transition is weakly first order. However, $(T_i - T^*)$ is notably small, in contrast to the large latent heat mentioned above.

Recently, the pseudocritical behavior below the transition temperature was discussed by Ikeda in the context of the Landau theory (16). The main term of the temperature dependence of $\langle \delta\eta^2 \rangle$ and τ is proportional to $\sqrt{T^{**} - T}$, in which T^{**} is a pseudocritical temperature in the gel phase. Solid lines below T_i in Fig. 6 represent the equations $\Delta = 5.43 \times 10^{-2}/\sqrt{41.4 - T}$, $\tau = 6.13 \times 10^{-8}/\sqrt{41.4 - T}$. The square-root dependence agrees very well with the experimental result. The relationship between the pseudocritical temperatures, T^* and T^{**} , is derived from the free energy, Eq. 12

$$T_i - T^* = 8(T^{**} - T_i). \quad (15)$$

Although we could not determine $(T^{**} - T_i)$ because of the scattering of the peak temperatures of various anomalies, Eq. 15 seems to be valid, because T^{**} is almost equal to T_i .

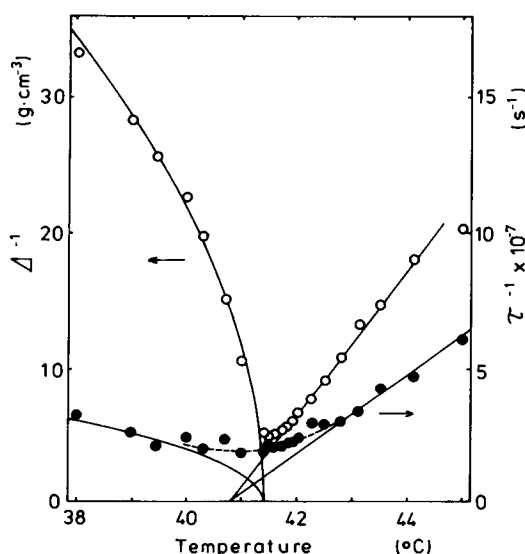


FIGURE 6 The reciprocals of relaxation strength (O) and relaxation time (●) as a function of temperature. Solid lines are drawn according to the Landau theory with the critical exponents of 1 for $T > T_i$ and 0.5 for $T < T_i$.

The large latent heat and the small value of $(T_i - T^*)$ seem to be the unique features of the gel-to-liquid crystal transition as clearly shown in Table I, in which the present results are summarized and compared with the corresponding values of the nematic-isotropic transition. The nematic-isotropic transition is a weak first-order transition that is characterized by an orientational order of long, rigid molecules. Most transition properties are similar for these systems: the magnitude of the relaxation time and strength, the critical exponents, $T_i - T^*$, and total change of density agree well for these transitions. However, the magnitude of the endothermic heat, most of which arises from the latent heat, is much larger in the gel-to-liquid crystal transition than in the nematic-isotropic transition. Therefore we conclude that the gel-to-liquid crystal transition includes many degrees of motional freedom, as previously discussed by Nagle (35).

As Stinson and Litster have done for the nematic-isotropic transition (36), we may calculate all the coefficients of the free energy, Eq. 12, by using the equations

$$Q = \frac{1}{2}aT_i\eta_i^2, \quad (16)$$

$$\eta_i = \frac{2A_3}{3A_4}, \quad (17)$$

$$T_i - T^* = \frac{2A_3^2}{9aA_4}. \quad (18)$$

Although we do not know the isothermal jump of the order parameter η_i , a reasonable value is 0.4 as estimated from the temperature dependence of the average orientational order parameter (37). Then the parameters are calculated from Eqs. 16–18; $a = 1.35 \text{ kJ/mol} \cdot \text{deg}$, $A_3 = 6.8 \text{ kJ/mol}$,

TABLE I
TRANSITION PROPERTIES OF LIPID BILAYERS AND NEMATICS

	DPPC	Nematics
Relaxation time (ns)	10–80	10–100*
Critical exponent ($T > T_i$)	1	1*
($T < T_i$)	0.5	0.4*
Relaxation strength		
$\Delta\kappa_m$ at T_i ($\text{cm}^2 \text{ dyn}^{-1}$)	1.5×10^{-11}	$\sim 5 \times 10^{-12}$ *
Critical exponent ($T > T_i$)	1	1*
($T < T_i$)	0.5	0.4*
$T_i - T^*$ ($^\circ\text{C}$)	~ 0.6	1‡
Total change of density (%)	3.5§	2–5
Total endothermic heat (kcal mol^{-1})	8.7¶	0.14**

*Reference 23.

‡Reference 36.

§Reference 2.

||References 40 and 41.

¶Reference 42.

**Reference 31.

and $A_4 = 10.1$ kJ/mol. The kinetic coefficient, ζ , in Eq. 14 is also determined to be 1.3 P, in accordance with the viscosities of lipid bilayer membranes (4, 22). However the coefficients, a , A_3 , and A_4 , are larger by factors of 10–50 than the values for the nematic-isotropic transition (36). The reason for this is simply the large latent heat of the gel-to-liquid crystal transition. When the coefficients of the free-energy expansion are increased by the same factor, most transition properties remain constant except the latent heat, as exemplified by Table I. The kinetics of the transition may also be influenced by the large coefficients, because the free-energy barrier between two phases becomes larger. Namely, hysteresis is observed in the transition region (7). We should not attach too much importance to the magnitude of the coefficients, however, because the applicability of Eq. 12 is still controversial. Many authors who employed similar expansions of the free energy have added the first-order term and some other terms (34, 38, 39). The present work provides at least the basic experimental requirements for all specific models of gel-to-liquid crystal transition.

We are grateful to Dr. K. Okano of the University of Tokyo, Dr. F. Jähnig of Max-Planck-Institut für Biologie, Tübingen, and S. Aruga of the Tokyo University of Agriculture and Technology for their valuable advice and discussions. We are also greatly indebted to Dr. I. Hatta of Nagoya University for his discussion in which the idea to use the Pippard's relationships was born.

Received for publication 18 October 1982 and in final form 14 January 1983.

REFERENCES

- Hinz, H.-J., and J. M. Sturtevant. 1972. Calorimetric studies of dilute aqueous suspensions of bilayer formed from synthetic L- α -lecithin. *J. Biol. Chem.* 247:6071–6075.
- Nagle, J. F. 1973. Lipid bilayer phase transition: Density measurements and theory. *Proc. Natl. Acad. Sci. USA.* 70:3443–3444.
- Lippert, J. L., and W. L. Peticolas. 1971. Laser Raman investigation of the effect of cholesterol on conformational changes in dipalmitoyl lecithin multilayers. *Proc. Natl. Acad. Sci. USA.* 68:1572–1576.
- Kawato, S., K. Kinosita, Jr., and A. Ikegami. 1978. Effect of cholesterol on the molecular motion in the hydrocarbon region of lecithin bilayers studied by nanosecond fluorescence technique. *Biochemistry.* 17:5026–5031.
- Seelig, A., and J. Seelig. 1974. The dynamic structure of fatty acyl chains in a phospholipid bilayer measured by deuterium magnetic resonance. *Biochemistry.* 13:4839–4845.
- Inoko, Y., and T. Mitsui. 1978. Structural parameters of dipalmitoylphosphatidylcholine lamellar phases and bilayer phase transitions. *J. Phys. Soc. Japan.* 44:1918–1924.
- Wu, E.-S., K. Jacobson, and D. Papahadjopoulos. 1977. Lateral diffusion in phospholipid multibilayers measured by fluorescence recovery after photobleaching. *Biochemistry.* 16:3936–3941.
- Shimshick, E. J., and H. M. McConnell. 1973. Lateral phase separation in phospholipid membranes. *Biochemistry.* 12:2351–2360.
- Mitaku, S., A. Ikegami, and A. Sakanishi. 1978. Ultrasonic studies of lipid bilayer. Phase transition in synthetic phosphatidylcholine liposomes. *Biophys. Chem.* 8:295–304.
- Mitaku, S. 1981. Ultrasonic studies of lipid bilayer phase transition. *Mol. Cryst. Liq. Cryst.* 70:1299–1306.
- Papahadjopoulos, D., K. Jacobson, S. Nir, and T. Isac. 1973. Phase transitions in phospholipid vesicles. Fluorescence polarization and permeability measurements concerning the effect of temperature and cholesterol. *Biochim. Biophys. Acta.* 311:330–348.
- Tsong, T. Y. 1977. Effect of phase transition on the kinetics of dye transport in phospholipid bilayer structures. *Biochemistry.* 16:2674–2684.
- Mitaku, S., and T. Date. 1982. Anomalies of nanosecond ultrasonic relaxation in the lipid bilayer transition. *Biochim. Biophys. Acta.* 688:411–421.
- Albrecht, O., H. Gruler, and E. Sackman. 1978. Polymorphism of phospholipid monolayers. *J. Physiol. (Paris).* 39:301–313.
- Landau, L. D., and E. M. Lifschitz. 1959. Statistical Physics. Trans. from Russian by J. B. Sykes and M. J. Kearsley. Pergamon Press, Ltd., London. 424–454.
- Ikeda, H. 1979. Pseudocritical dynamics in first-order transitions. *Progr. Theor. Phys.* 61:1023–1033.
- Pippard, A. B. 1956. Thermodynamic relations applicable near a λ -transition. *Phil. Mag.* 1:473–476.
- Stanley, H. E. 1971. Introduction to Phase Transitions and Critical Phenomena. Oxford University Press, London. Trans. into Japanese by K. Matsuno Tokyo Tosho Co., Tokyo. 257.
- Jähnig, F. 1979. Molecular theory of lipid membrane order. *J. Chem. Phys.* 70:3279–3290.
- Mitaku, S., T. Jippo, R. Kataoka, and T. Date. 1982. Critical slowing down in lipid bilayer membrane studied by a differential ultrasonic resonator. *Jap. J. Appl. Phys.* 21(Suppl.)21–3:77–79.
- Eggers, F., and T. Funck. 1973. Ultrasonic measurements with milliliter liquid samples in the 0.5–100 MHz range. *Rev. Sci. Instrum.* 44:969–977.
- Mitaku, S., and K. Okano. 1981. Ultrasonic measurements of two-component lipid bilayer suspensions. *Biophys. Chem.* 14:147–158.
- Eden, D., C. W. Garland, and R. C. Williamson. 1973. Ultrasonic investigation of the nematic-isotropic phase transition in MBBA. *J. Chem. Phys.* 58:1861–1868.
- Sheets, M. P., and S. I. Chan. 1972. Effect of sonication on the structure of lecithin bilayers. *Biochemistry.* 11:4573–4581.
- Suurkuusk, J., B. R. Lentz, Y. Barenholtz, R. L. Biltonen, and T. F. Thompson. 1976. A calorimetric and fluorescent probe study of the gel-to-liquid crystalline phase transition in small single-lamellar dipalmitoylphosphatidylcholine vesicles. *Biochemistry.* 15:1393–1401.
- Doniach, S. 1978. Thermodynamic fluctuations in phospholipid bilayers. *J. Chem. Phys.* 68:4912–4916.
- Nagle, J. F., and H. L. Scott, Jr. 1978. Lateral compressibility of lipid mono- and bilayers. Theory of membrane permeability. *Biochim. Biophys. Acta.* 513:236–243.
- Wilks, J. 1967. The Properties of Liquid and Solid Helium. Clarendon Press, Oxford. 289.
- Trudell, J. R., D. G. Payan, J. H. Chin, and E. N. Cohen. 1974. Pressure-induced elevation of phase transition temperature in dipalmitoylphosphatidylcholine bilayers. *Biochim. Biophys. Acta.* 373:436–443.
- Wilkinson, D. A., and J. F. Nagle. 1982. Specific heats of lipid dispersions in single phase regions. *Biochim. Biophys. Acta.* 688:107–115.
- Arnold, V. H. 1964. Kalorimetrie kristallin-flüssiger Substanzen II. Resultate der Messungen an 12 homologen Dialkoxy-Azoxybenzenen. *Z. Phys. Chem.* 226:146–156.
- De Gennes, P. G. 1974. The Physics of Liquid Crystals. Clarendon Press, Oxford. 347.
- Kawamura, Y., Y. Maeda, K. Okano, and S. Iwayanagi. 1973. Anomalous ultrasonic absorption and dispersion of nematic liquid

- crystals near the clearing point. *Jap. J. Appl. Phys.* 12:1510–1521.
34. Jähnig, F. 1981. Critical effects from lipid-protein interaction in membranes. I. Theoretical description. *Biophys. J.* 36:329–345.
 35. Nagle, J. F. 1980. Theory of the main lipid bilayer phase transition. *Annu. Rev. Phys. Chem.* 31:157–195.
 36. Stinson, T. W., III, and J. D. Litster. 1970. Pretransitional phenomena in the isotropic phase of nematic liquid crystal. *Phys. Rev. Lett.* 25:503–506.
 37. Jähnig, F. 1979. Structural order of lipids and proteins in membranes: Evaluation of fluorescence anisotropy data. *Proc. Natl. Acad. Sci. USA.* 76:6361–6365.
 38. Owicki, J. C., N. W. Springgate, and H. M. MacConnell. 1978. Theoretical study of protein-lipid interactions in bilayer membrane. *Proc. Natl. Acad. Sci. USA.* 75:1616–1619.
 39. Izuyama, T., and Y. Akutsu. 1982. Statistical mechanics of biomembrane phase transition II. The first order transition with pseudocritical properties. *J. Physiol. Soc. Japan.* 51:730–740.
 40. Chistiyakov, I. G. 1967. Liquid crystals. *Sov. Phys. Usp.* 9:551–573.
 41. Troza, S., and P. E. Cladis. 1974. Volumetric study of the nematic-smectic-A transition of *n-p*-cyanobenzylidene-*p*-octyloxyaniline. *Phys. Rev. Lett.* 32:1406–1409.
 42. Albon, N., and J. M. Sturtevant. 1978. Nature of the gel to liquid crystal transition of synthetic phosphatidylcholine. *Proc. Natl. Acad. Sci. USA.* 75:2258–2260.